Comprehensive Atmospheric Modeling of Reactive Cyclic Siloxanes and Their Oxidation Products

Nathan J. Janechek[1,2], Kaj M. Hansen[3], and Charles O. Stanier[1,2]

[1]Department of Chemical and Biochemical Engineering, University of Iowa, Iowa City, IA 52242, USA
[2]IIHR Hydroscience and Engineering, University of Iowa, Iowa City, IA 52242, USA
[3]Department of Environmental Science, Aarhus University, Roskilde, Denmark

Correspondence to: Charles O. Stanier (charles-stanier@uiowa.edu)

Abstract. Cyclic volatile methyl siloxanes (cVMS) are important components in personal care products that transport and react in the atmosphere. Octamethylcyclotetrasiloxane (D_4), decamethylcyclopentasiloxane (D_5), dodecamethylcyclohexasiloxane (D_6), and their gas phase oxidation products have been incorporated into the Community Multiscale Air Quality (CMAQ) model. Gas phase oxidation products, as the precursor to secondary organic aerosol from this compound class, were included to quantify the maximum potential for aerosol formation from gas phase reactions with OH. Four 1-month periods were modeled to quantify typical concentrations, seasonal variability, spatial patterns, and vertical profiles. Typical model concentrations showed parent compounds were highly dependent on population density as cities had monthly averaged peak D_5 concentrations up to 432 ng m^{-3}. Peak oxidized D_5 concentrations were significantly less, up to 9 ng m^{-3} and were located downwind of major urban areas. Model results were compared to available measurements and previous simulation results. Seasonal variation was analyzed and differences in seasonal influences were observed between urban and rural locations. Parent compound concentrations in urban and peri-urban locations were sensitive to transport factors, while parent compounds in rural areas and oxidized product concentrations were influenced by large-scale seasonal variability in OH.

1 Introduction

Cyclic volatile methyl siloxanes (cVMS) are present in a wide range of personal care and cosmetic products (e.g. hair products, lotions, antiperspirants, makeup, and sunscreens) as well as in sealers, cleaning products, and silicone products (Wang et al., 2009; Horii and Kannan, 2008; Dudzina et al., 2014; Lu et al., 2011; Capela et al., 2016). As high production volume chemicals (>1,000 tonne yr^{-1} produced) (OECD Environment Directorate, 2004), their environmental fate is an important topic. The most prevalent cVMS species in personal care products is decamethylcyclopentasiloxane (D_5), although octamethylcyclotetrasiloxane (D_4) and dodecamethylcyclohexasiloxane (D_6) are also emitted (Horii and Kannan, 2008; Dudzina et al., 2014; Wang et al., 2009; Lu et al., 2011). Atmospheric lifetimes (Atkinson, 1991) are approximately 5-10 days at typical OH concentrations; accordingly, long-range transport (Xu and Wania, 2013; Krogseth et al., 2013a; McLachlan et al., 2010; Genualdi et al., 2011; MacLeod et al., 2011) of cVMS occurs. The environmental fate and transport of cVMS has

been widely studied due to concerns of potential persistent, bioaccumulative, and toxic (PBT) behavior in the environment, however assessing the environmental risk has been a subject of debate due to unique cVMS properties, evolving scientific information on properties and presence in the environment, and different interpretations of risk assessment information. The parent cyclic siloxanes have been the subject of a number of regulatory screenings including those by Canada (Environment Canada and Health Canada, 2008a, b, c), the UK (Brooke et al., 2009b, a, c), and the EU (ECHA, 2015); comprehensive review articles (Rucker and Kummerer, 2015; Wang et al., 2013) and recent environmental fate studies (Mackay et al., 2015; Gobas et al., 2015a; Gobas et al., 2015b; Fairbrother et al., 2015) are also relevant. The conceptual model of cVMS fate and transport is summarized as emission (mainly to the atmosphere) in population centers as a result of personal care product (PCP) use (Mackay et al., 2015; Montemayor et al., 2013; Gouin et al., 2013), followed by atmospheric transport and reaction by the hydroxyl radical (OH) (Xu and Wania, 2013). Emissions and concentrations are highly dependent on population, with urban locations (Yucuis et al., 2013; Genualdi et al., 2011; Krogseth et al., 2013b; Buser et al., 2013a; Companioni-Damas et al., 2014; Ahrens et al., 2014) and indoor environments (Tang et al., 2015; Yucuis et al., 2013; Companioni-Damas et al., 2014; Pieri et al., 2013; Tri Manh and Kannan, 2015) having much higher concentrations than remote locations. As this work shows, the population-dependent PCP emissions are best validated for D_5, and the importance of other emission types, and the variation of this by cVMS compound, is uncertain.

Substantial insights regarding cVMS fate, transport, and expected concentrations have come from atmospheric modeling studies. McLachlan et al. (2010) simulated atmospheric D_5 concentrations using the Danish Eulerian Hemispheric Model (DEHM), a hemispheric scale 3D atmospheric chemistry and transport model. MacLeod et al. (2011) simulated D_5 globally using the Berkeley-Trent Global Model (BETR Global), a multimedia mass balance model at 15° horizontal resolution. Global zonally averaged modeling using the multimedia GloboPop model has also been performed (Xu and Wania, 2013; Wania, 2003). Emission estimates have been back-calculated from measured atmospheric concentrations using a multimedia model (Buser et al., 2013a; Buser et al., 2014), and compartmental model studies focusing on specific partitioning or loss processes have also been conducted (Navea et al., 2011; Whelan et al., 2004). These modeling studies have permitted extension, both in time and space, beyond the sparse measurement dataset and testing of key model processes (emissions, fate, and transport) versus modeled concentrations. Latitudinal gradients, urban-rural-remote gradients, seasonal patterns, sensitivity to processes and parameterizations, and diel cycles have been explored using these models. Modeling studies have shown the large scale concentration patterns with OH as a dominant loss process, and quantified the importance of the atmosphere (relative to sediment and surface waters) for fate and transport. Seasonal and latitudinal trends can be explained in part by availability of OH. Models estimate D_5 concentrations of 50 ng m^{-3} and higher in well-mixed urban air (Navea et al., 2011), while 0.04 to 9 ng m^{-3} is reported from models for remote locations (Krogseth et al., 2013a).

Atmospheric measurements of cyclic siloxanes have been performed in ambient air (McLachlan et al., 2010; Genualdi et al., 2011; Yucuis et al., 2013; Ahrens et al., 2014; Kierkegaard and McLachlan, 2013; Krogseth et al., 2013b; Krogseth et al., 2013a; Buser et al., 2013a; Companioni-Damas et al., 2014). Higher concentration microenvironments have also been surveyed through measurement (WWTP, landfills, and indoor air) (Krogseth et al., 2013b; Cheng et al., 2011; Wang et al.,

2001; Pieri et al., 2013; Yucuis et al., 2013; Tri Manh and Kannan, 2015; Companioni-Damas et al., 2014; Tang et al., 2015). In several instances, model-measurement comparison has been conducted and to a large extent, confirmed our understanding of emissions, fate and transport. Generally good agreement for rural and remote locations have been observed (McLachlan et al., 2010; Krogseth et al., 2013a; MacLeod et al., 2011; Navea et al., 2011; Xu and Wania, 2013; Genualdi et al., 2011) while urban areas tend to be under predicted (Genualdi et al., 2011; Yucuis et al., 2013; Navea et al., 2011). Measured seasonal concentration variations have been replicated for sites in rural Sweden and the remote Arctic. However, it was noted that the DEHM model tended to have better agreement during late spring (McLachlan et al., 2010) and late summer (Krogseth et al., 2013a) compared to winter. The BETR model conversely had better agreement during winter compared to late spring for the same rural Sweden site (MacLeod et al., 2011).

The majority of modeling and chamber study investigation, and all of the ambient measurements for cVMS, have focused on the emitted or "parent" cVMS compounds (i.e., D_4, D_5, and D_6). The identity and fate of the cVMS oxidation products has received less scrutiny until recently, compared to the parent compounds. Sommerlade et al. (1993) reacted D_4 with OH in an environmental chamber and identified multiple reaction products by GC-MS, with the single OH substituted silanol (D_3TOH) as the most prevalent resolved species, with species identification confirmed by matching retention time and mass spectra compared to synthesized D_3TOH. Because of the method of collection (the product was collected from rinsing the environmental chamber walls with solvent) confirmation of secondary aerosol production from D_4 oxidation was not possible from Sommerlade et al. (1993). Chandramouli and Kamens (2001) reacted D_5 in a smog chamber, with separate analysis of gas and aerosol products, confirming the presence of D_4TOH in the GS/MS analysis of the condensed aerosol phase.

Wu and Johnston (2016) conducted more exhaustive characterization of aerosols from photooxidation of D_5, using high performance mass spectrometry, revealing both monomeric and dimeric oxidation products, with molar masses up to 870. Oxidation progressed not only by substitution of a methyl group with OH (e.g. leading to D_4TOH), but also by substitution with CH_2OH; linkages between Si-O rings to form dimers were through O, CH_2, and CH_2CH_2 linkage groups.

Aerosols containing Si and likely from photooxidation of gaseous precursors have been recently identified in multiple locations in the U.S. using laser ablation particle mass spectrometry of ultrafine particles (Bzdek et al., 2014). Bzdek et al. (2014) contend that a photooxidation source is most consistent with observations because of the times of day of occurrence, short atmospheric lifetime of the particle size in question (10-30 nm), lack of wind direction dependence that would be expected from primary sources, ubiquity across disparate measurement sites, and similarity in temporal evolution of nanoaerosol Si to other species with known photochemical sources. Except for the reports of the concentrations of ambient oxidized cVMS in Bzdek et al. (2014), there are no ambient measurements or model-based estimates of the potential aerosol concentrations from cVMS oxidation. This work begins to address that gap by simulating the gas phase oxidation product concentrations using the atmospheric chemistry and transport model Community Multiscale Air Quality (CMAQ). As experimental determinations of aerosol yield become available, the simulations can be updated to include secondary organosilicon aerosol concentrations.

This work builds on the limited information available on the oxidation products. Properties relevant to fate and transport (e.g. Henry's law coefficient) have been predicted in this work and in others based on structure activity relationships (Buser et al., 2013b; Whelan et al., 2004). Latimer et al. (1998) measured equilibrium gas particle partitioning of D_5 and D_4TOH on diesel, wood, coal soot, and Arizona fine dust aerosols. Whelan et al. (2004) performed equilibrium air-particle and air-cloud droplet partitioning modeling of multiple substituted OH silanols. More extensive information is available about the gas-particle partitioning (Latimer et al., 1998; Tri Manh and Kannan, 2015; Tri Manh et al., 2015; Kim and Xu, 2016) and aerosol phase reactions (Navea et al., 2011; Navea et al., 2009a; Navea et al., 2009b) of the precursor compounds, but these confirm that the gas-phase oxidation and transport of the parent compounds are substantially more important than the heterogeneous oxidation pathways and thermodynamic partitioning of the parent compounds onto ambient aerosols.

In this work, atmospheric gas phase concentrations of D_4, D_5, D_6, and its oxidization products are modeled comprehensively using the chemical transport CMAQ model. The purpose of the model-based investigation is twofold. First, it enables the highest resolution (36 km) to-date simulation of the parent compound over the U.S.; the model simulates vertical profiles, urban-to-rural transitions, and the dependence of these on factors such as season and mixed layer height. Second, this paper reports, for the first time in detail, concentrations of the cVMS oxidation products. Some fraction of products is likely distributed into the aerosol phase, thus contributing to aerosol Si concentrations on regional and global scales. We expand upon the modeling first presented in Bzdek et al. (2014), but with improved emission estimates, inclusion of wet and dry deposition, and incorporation of season-dependent boundary conditions.

2 Methods

Cyclic siloxanes and oxidized cyclic siloxanes were modeled with the 3D atmospheric chemical transport model CMAQ (Byun and Schere, 2006) modified to include cyclic siloxane species. CMAQ version 4.7.1 was used and the modeling domain covered the contiguous U.S., northern Mexico, and southern Canada. The domain had 14 vertical layers and a horizontal resolution of 36 km. Four, one-month simulations were performed for January, April, July, and October to characterize seasonal variability of cyclic siloxane atmospheric concentrations. A spin up period of 7 days was used to minimize the influence of zero initial conditions for the cyclic siloxanes species. Meteorology was from the Weather Research and Forecasting (WRF) model version 3.1.1 for the meteorological year of 2004. WRF was run with time steps of 120 s, 30 vertical layers, Morrison double-moment microphysics scheme, RRTMG longwave and shortwave physics scheme, Pleim-Xiu surface layer, Pleim-Xiu land surface model with two soil layers, and the ACM2 PBL scheme. Reanalysis nudging using North American Regional Reanalysis (NARR) data was performed every three hours.

The cyclic siloxanes were added to the CMAQ model by adding D_4, D_5, D_6, and the oxidized species, o-D_4, o-D_5, and o-D_6 to the cb05cl_ae5_aq mechanism. Rate constants for the parent cyclic siloxanes reacting with hydroxyl radicals (OH) were used from Atkinson (1991) where D_4 and D_5 were determined experimentally and D_6 estimated from the reported D_5 per methyl rate. The rate constants used were 1.01×10^{-12}, 1.55×10^{-12}, and 1.92×10^{-12} cm^3 molecule^{-1} s^{-1} for D_4, D_5, and D_6,

respectively. Reactions of the oxidation products are not included in the model. In part, this is because information is limited on the kinetics of further oxidation and on the changes that this would cause for fate, transport, and properties. Whelan et al. (2004) modeled subsequent oxidation reactions, and chamber-based oxidation studies observe multiple substitution products likely due to multiple substitution reactions or auto-oxidation by internal rearrangement (Wu and Johnston, 2016). In the model, only the first oxidation is computed. The oxidation products are denoted o-D_4, o-D_5, and o-D_6, and for calculation of physical properties relevant to deposition, the single OH substitution is assumed.

Wet and dry deposition of the primary species (e.g. D_4, D_5) were added to the model using Henry's law coefficients (Xu and Kropscott, 2012). For the oxidized cyclic siloxanes, physicochemical parameters were estimated using EPI Suite HENRYWIN v3.20 (EPA, 2012) for the single OH substitution of one methyl group of the parent cyclic siloxane (e.g., D_3TOH, D_4TOH). Deposition related inputs necessary for the CMAQ deposition routine included Henry's law coefficients, mass diffusivities, reactivity, and mesophyll resistance. CMAQ calculates dry deposition as a deposition velocity (dependent on mixing/turbulence, molecular properties, and land type) multiplied by the lowest model layer concentration (Byun et al., 1999), and wet deposition using Henry's law coefficients and precipitation rates (Roselle and Binkowski, 1999). Dry deposition therefore treats the surface as an infinite sink, which is consistent with other species in the model. The mass diffusivity values were calculated by the Fuller, Schettler, and Giddings (FSG) method (Lyman et al., 1982) where molar volume was estimated based on element contributions. Sulfur molar volume contribution values were substituted for silicon atoms since silicon values were not available. Calculated mass diffusivity values, as estimated by the FSG method were 0.0512 (D_4), 0.0454 (D_5), 0.0411 (D_6), 0.0527 (o-D_4), 0.0464 (o-D_5), and 0.0419 (o-D_6) cm^2 s^{-1}. The reactivity parameter was set at 2.0 in common with methanol and other species of limited reactivity. The mesophyll resistance, which is used to account for uptake by plants, was set to zero (only a few species had mesophyll resistances specified in CMAQ, such as NO_2, NO, CO, and Hg gas). Molecular weight for the oxidized cyclic siloxanes assumed the single substituted OH species. The molecular weight of D_6 and o-D_6 exceeded the limit of the CMAQ dry deposition routine m3dry (390 g mol^{-1}) and values in excess of the limit were coerced to the limit. The impact of this substitution is expected to be minimal, since it is a minor adjustment to a minor pathway; dry deposition of cVMS is relatively small (McLachlan et al., 2010; Xu and Wania, 2013; Whelan et al., 2004).

Emissions of cyclic siloxanes were distributed according to gridded population for the U.S., Canada, and Mexico while Caribbean countries were neglected. The U.S., Canadian, and Mexican per capita emission rates of D_5 provided by personal communication (van Egmond, 2013) and previously used and reported in McLachlan et al. (2010) was adopted for this study. Briefly, as reported in McLachlan et al. (2010), D_5 emission rates were derived from country specific market share based on antiperspirant sales data combined with D_5 consumption data from antiperspirant plus 10% to account for other sources. A table of many available cVMS emissions rates from multiple methods are represented in Table S2, and a wide variation exists. To calculate D_4 and D_6 emission rates, ambient measurements from Chicago (Yucuis et al., 2013) were used to estimate emission ratios relative to D_5. Chicago was chosen since it is a major urban area and atmospheric measurements should be most fresh and therefore the best representation of emission rates. However, since OH reactivity (and other fate and transport properties) vary from compound to compound, ambient measurements of compound ratios will not match emission

ratios, except in air parcels that are so fresh as to have seen no oxidation. To check for the influence of air mass aging in the measurements of Yucuis et al. (2013), the ratio NO_x/NO_y was used as a marker of air mass age (Slowik et al., 2011). This ratio is high in fresh emissions, and decreases as the air mass is oxidized. Hourly measurements of NO_x and NO_y from Northbrook, Illinois (EPA) were inspected during the time period of the Chicago sampling in Yucuis et al. (2013). Using the

5   NO_x/NO_y photochemical age estimate, we calculated that emitted ratios vs. ambient ratios likely differed by less than 1% (see Supplemental section). The Chicago cyclic siloxane measurements were therefore used as emission ratios without photochemical age correction. The resulting emission ratios, 0.243 and 0.0451 for D_4/D_5 and D_6/D_5 respectively, were multiplied by the D_5 emission rate to estimate the D_4 and D_6 emission rates. The resulting D_4, D_5, and D_6 country emission rates, which were constant for all simulations, were multiplied by gridded population and merged with Sparse Matrix Operator

10   Kernel Emissions (SMOKE) model version 2.5 generated year 2004 emissions. Population data was from census derived population surrogates from EPA 2011 v6.0 Air Emissions Modeling Platform and is based on permanent residency and does not include seasonal tourism. This may cause inaccuracies in emissions near parks and other tourist destinations. SMOKE emissions were calculated from NEI 2002, version 3, with on-road and point sources projected to 2004 using EGAS, the EPA's Point source and Economic Growth Analysis System. Biogenic emissions were from BEIS 3.13.

15   Boundary conditions were from previous DEHM modeling that modeled D_5 concentrations using 2009 emission rates as described above (Hansen et al., 2008; McLachlan et al., 2010). The DEHM model was run for the Northern Hemisphere at 150 km resolution. We extracted the D_5 concentrations from the DEHM model for year 2011 meteorology along our model boundary. Boundary concentrations were horizontally and vertically resolved, varied by month, but were time invariant within each month. Since the DEHM model only included D_5, D_4 and D_6 concentrations were estimated using measurement ratios

20   taken from a background site at Point Reyes, CA (Genualdi et al., 2011). Point Reyes samples had ratios of 0.646 and 0.0877 for D_4/D_5 and D_6/D_5 respectively. The background ratios combined with the "fresh" emission ratios (described previously) were used to calculate a photochemical age. The calculation of a photochemical age was necessary since the siloxanes have different OH reaction rates and therefore the siloxane ratios change with season due to varying OH concentrations. Using this method, we calculated an age of 17.6 days using the D_4/D_5 ratios and this is the age used for further calculations. The calculated

25   photochemical age was combined with season specific OH concentrations (Spivakovsky et al., 2000) to calculate monthly resolved D_4/D_5 and D_6/D_5 "background" ratios. These monthly resolved D_4/D_5 and D_6/D_5 ratios were then used for the entire model boundary. Additional details are available in the Supplemental section.

3 Results and Discussion

3.1 Spatial Variation in Concentrations

30   Figures 1 and 2 show the 30 day averaged D_5 and oxidized D_5 (o-D_5) modeled concentrations for January, April, July, and October. The spatial distribution of cVMS and oxidized cVMS compounds show a strong population dependence with major urban areas having elevated D_5 concentrations and peak o-D_5 concentrations occurring hundreds of km downwind of source

regions due to the time it takes for the parent compounds to react with OH. Table 1 displays the monthly minimum, maximum, and average concentrations for the entire modeled domain. The 36-km grid cell with the highest 30-day average surface concentration of D_5 was 432, 379, 301, and 265 ng m^{-3} for January (Los Angeles – Long Beach), April (Los Angeles – Long Beach), October (New York City), and July (New York City), respectively. The domain-averaged surface concentrations of D_5 were 6.82, 6.43, 5.09, and 4.04 ng m^{-3} for January, October, April, and July. Simulated o-D_5 was much lower than simulated D_5 concentrations. For example, the 36-km grid cell with the highest 30-day average surface concentration of o-D_5 was 9.04, 5.21, 4.86, and 3.19 ng m^{-3} for July (NE of Los Angeles – Victorville), October (E of Los Angeles – San Bernardino), April (SE of Los Angeles – Mission Viejo), and January (Los Angeles – Long Beach), respectively. The domain average surface concentration for o-D_5 was 0.81, 0.72, 0.63, 0.37 ng m^{-3} for July, April, October, and January, respectively. The peak domain-averaged concentrations occurred during January for D_5 and July for o-D_5 which is expected based on seasonal trends of OH in North America (Spivakovsky et al., 2000).

Figure 3 shows the monthly averaged cVMS and oxidized cVMS concentrations versus the model grid cell population for 26 U.S. and Canadian sites. These sites include the most populous ten U.S. metropolitan areas, siloxane measurement sites, and NOAA Climate Monitoring and Diagnostics Laboratory (CMDL) sites, see Table S3 for the full list. Modeled concentrations are strongly dependent on population with New York City and Los Angeles having the highest concentrations (Table S4). In addition to the population dependence, concentrations were greatest for D_5 followed by D_4 and D_6. This follows from our assumed emission ratios and agrees with North American measurement data (Yucuis et al., 2013; Genualdi et al., 2011; Ahrens et al., 2014; Krogseth et al., 2013b). The prevalence of D_4 relative to D_6 is of interest because analysis of cVMS composition in consumer products (Horii and Kannan, 2008; Wang et al., 2009; Dudzina et al., 2014; Lu et al., 2011; Capela et al., 2016) suggests that D_6 is more abundant than D_4 – while in our modeling (and atmospheric measurements) D_4 concentrations are higher than D_6 concentrations. Four explanations bear further investigation: (1) non-personal care emissions (e.g. cVMS residuals from polymer production) may play a more important role for D_4 than other species based on UK emission estimates (Brooke et al., 2009b, a, c), (2) possible siloxane conversion during sample collection (Kierkegaard and McLachlan, 2013; Krogseth et al., 2013a), (3) higher D_4 volatility (Lei et al., 2010) could cause both more difficult detection in personal care products and a larger fraction volatilization from products, and (4) uncertainty and/or spatiotemporal variability in the D_4/D_5 and D_6/D_5 ratios from ambient measurements in Chicago used to extend the D_5 emissions estimates to D_4 and D_6.

3.2 Seasonal Variation in Concentrations

Since OH concentrations vary seasonally we expect higher cVMS in the winter (low OH) and lower in the summer (high OH). This has been supported by previous measurement studies. For example, McLachlan et al. (2010) measured D_5 at a rural site in Sweden (59°N) and observed reduced D_5 concentrations for the period of May-June compared to January-April. Measurements in a remote Artic location (79°N) observed higher concentrations in the winter compared to late summer (Krogseth et al., 2013a). For OH concentrations to influence cVMS concentrations, time for oxidation is required – so the relationship between seasonal OH and cVMS is expected at receptor sites where most cVMS is transported from upwind

locations. At source-dominated locations, the influence of OH should be limited. For example, studies from Toronto highlight local meteorological influences as important in determining variation in siloxane (D_3-D_6) concentrations (Ahrens et al., 2014; Krogseth et al., 2013b).

Figure 1 shows similar D_5 spatial distribution between the four months, especially for urban areas. Domain peak and average concentrations (Table 1) have highest concentrations in January and lowest in July which agree with seasonal OH concentrations but specific grid cells (particularly urban locations) often deviate from this. Rural and remote locations are more likely to follow the OH-induced seasonal pattern. Seasonal variation for the 26 sites in Table S3 was examined using the most prevalent month, highest concentrations occurred. Sites were classified as either urban or rural based on summer D_5 concentrations. For urban sites, the most prevalent month with highest average D_5 concentration was October (59%), followed by July (23%), and January (18%). Restricting the analysis to the rural sites (summer D_5 concentration below 17 ng m^{-3}), peak D_5 concentrations occurred in January (56%), followed by October (33%), and April (11%). The month of lowest average D_5 concentrations occurred in July for 100% of the rural sites and 24% of the urban sites. Similarly, looking at the breakdown for the monthly averaged oxidized D_5 concentrations, highest concentrations generally occurred in July, which was true for 73% of the 26 sites. Figure 2 shows differences in the spatial distribution of o-D_5 between months. The analyzed sites therefore suggest less of a seasonal trend for the parent compounds as compared to the oxidized products, and there are differences in seasonal trends between source and non-source locations. Remote and rural sites are more dependent on lifetime with respect to reaction with OH, while source locations are less sensitive. This agrees with previous modeling which showed reduced seasonal variability of D_5 concentrations for urban areas compared to remote locations (McLachlan et al., 2010; MacLeod et al., 2011; Xu and Wania, 2013).

Statistical relationships between D_5, OH, planetary boundary layer (PBL) height, and wind speed (WS) were explored using least squares multiple linear regression. For the 26 analyzed sites, OH, PBL, and WS values were normalized to their summer values and then used as predictive variables of the ratio of D_5 in each season to its summer value at the same site. In other words, the regression analysis is testing the local season-to-season variability across seasons and sites (e.g. is winter:summer D_5 concentration correlated to winter:summer OH^{-1}). Sites were split between urban and rural as described previously. For urban sites, D_5 concentration was only correlated to OH^{-1} when WS^{-1} was also included, with WS being the dominant variable. The strongest predictive variables were PBL^{-1} and WS^{-1} with an adjusted R^2 fit of 0.50 and a p-value of <0.001. The regression analysis supports the previous conclusion: ventilation of local emissions through PBL height and local winds is the strongest influence on urban siloxane concentrations.

For the rural sites, WS^{-1} was the only variable of significance but had a low adjusted R^2 of 0.10, p-value of 0.056, and a negative coefficient meaning lower wind speed results in lower D_5 concentrations. Repeating the linear regression excluding Canadian sites and Point Reyes (CA), led to similar results. Canadian sites were excluded since non-siloxane Canadian emissions were allocated by population and may cause errors in OH due to misallocation of nitrogen oxides and reactive organic gases from some source sectors (Spak et al., 2012). Point Reyes was excluded due to high grid cell population despite low D_5 concentrations. See the Supplemental section for additional regression results. From this analysis, we conclude that

8

factors other than local OH and local meteorology control rural/remote siloxane concentrations. These factors likely include regional OH and regional transport patterns.

3.3 Model-Measurement Comparison

The model results were compared to measurement values in the Midwest (Yucuis et al., 2013), North American measurements from the Global Atmospheric Passive Sampling (GAPS) network (Genualdi et al., 2011), and several Toronto measurements (Genualdi et al., 2011; Ahrens et al., 2014; Krogseth et al., 2013b).

3.3.1 Midwest Model Comparison

In Yucuis et al. (2013) measurements were taken at three Midwest locations during the summer (June-August) of 2011. The measurements were collected, in duplicate, at sites with varying population density. Measurements from Chicago, IL were collected consecutively as sixteen 12 h samples from August 13 – 21, Cedar Rapids, IA as four 24 h samples non-consecutively from June 29 – July 26, and West Branch, IA as five samples that ranged from 30 – 47 h July 6 and consecutively from July 15 – 22. The measurements were compared to the July 1 – 30 modeled hourly concentrations averaged as 12, 24, and 36 h intervals for the Chicago, Cedar Rapids, and West Branch sites respectively. These sampling periods and sample counts are insufficient to establish representativeness of the values as monthly or seasonal averages. The model results were averaged using time-of-day and duration matching the measurements, but do not correspond to the exact measurement days or meteorology. Measurements are from 2011 and the model's meteorological fields are from 2004; however, average wind speeds, wind directions, and boundary layer heights are typically similar from year to year.

Figure 4 displays the boxplot comparison of the three Midwest sites of Yucuis et al. (2013) and the modeled concentrations. The model does capture the population dependence that the measurements show, with Chicago observing highest concentrations followed by Cedar Rapids and West Branch. Modeled concentrations however are lower for all three locations compared to the measurements with fractional bias (Table S10) at Chicago of -0.31, -0.31, -0.28 (for D_4, D_5, D_6 respectively), Cedar Rapids -1.25, -0.93, -1.51, and West Branch -1.25, -0.78, -1.23. Comparing the relative percent error of the mean modeled concentrations to the measured values, Chicago sites had relative percent errors of around 25% while the other sites had values ranging from 56% - 86%. For Chicago, error between the species was similar and this is most likely the result that D_4 and D_6 emission rates were calculated based on the Chicago measurements. For Cedar Rapids and West Branch, D_5 had the lowest error while D_4 and D_6 were larger. This may indicate that the siloxane emission ratios vary based on location.

One possible explanation for low model concentrations could be low emission estimates. Current emission estimates (Table S2) vary considerably and the estimates used in this work were 32.8, 135, and 6.10 mg person^{-1} day^{-1} for D_4, D_5, and D_6 respectively for the U.S. and Canada, while the Mexico emissions were 5.92, 24.4, and 1.10 mg person^{-1} day^{-1} for D_4, D_5, and D_6. Previous emission estimates have ranged from 0.001 – 100, 0.002 – 1200, and 0.0009 – 80 mg person^{-1} day^{-1} for D_4, D_5, and D_6 respectively (Tang et al., 2015; Buser et al., 2013a; Buser et al., 2014; Navea et al., 2011; Yucuis et al., 2013; Horii and Kannan, 2008; Dudzina et al., 2014; Wang et al., 2009; Capela et al., 2016). Additionally, non-personal care product

emissions could be important, as could potential geographical, demographical, or temporal influences on siloxane emissions. As datasets of cVMS concentrations, particularly those with simultaneous values for D_4, D_5 and D_6 are available in more source-oriented locations and seasons, the emissions estimates, particularly for D_4 and D_6, should be refined.

The treatment of deposition as an infinite sink could also cause low gas phase concentrations (deposition overpredicted) if surface concentration are not degraded quickly. Experimental studies show the parent cVMS degradation is slow in soil (Wang et al., 2013), however this is likely minimized due to low deposition potential as predicted by high air-water (K_{AW}) and low octanol-air (K_{OA}) partitioning coefficients (Xu and Wania, 2013). Octanol-air ($logK_{OA}$) partitioning values, which is an indication of the ability to partition to soil and plants (Shoeib and Harner, 2002), are $4.29 - 5.86$ for D_4-D_6 (Xu and Kropscott, 2012), which is similar or higher than other organic species with modeled deposition such as methanol, aldehydes, and carboxylic acids. The oxidized species are likely more sensitive due to greater deposition potential as EPI Suite predicts lower $logK_{AW}$ and higher $logK_{OA}$ values, however the surface degradation kinetics of the oxidation products are not known.

3.3.2 GAPS Model Comparison

The model was also compared to measurements of Genualdi et al. (2011). These measurements were collected from passive samplers as part of the GAPS network over three months in 2009, generally from late March to early July. Figure 5 shows the CMAQ modeled April month versus measurements for eight locations within our domain. Again as with the Yucuis et al. (2013) comparison, the modeled results do not explicitly represent meteorological conditions of the measurement period. Fractional error (Table S11) for D_4 varied from $0.02 - 1.93$ with Point Reyes having the lowest and Ucluelet the highest. For D_5, fractional error values ranged from $0.02 - 1.24$ with Fraserdale the lowest and Bratt's Lake the highest. Similarly, for D_6, the fractional error varied from $0.11 - 1.71$ with Bratt's Lake the lowest and Ucluelet the highest. Averaged over the eight sites, the overall fractional biases were -0.41, -0.03, and -0.90 for D_4, D_5, and D_6, respectively. The mean fractional error was 0.95, 0.66, and 0.98 for D_4, D_5, and D_6 species. Therefore, based on the fractional error values, D_5 had the best agreement followed by D_4 and D_6. This is not surprising that D_5 had the best agreement since D_4 and D_6 emission rates are estimated based on Chicago measurements and would have additional uncertainty compared to the D_5 emission uncertainty.

On average, fractional bias for D_5 was close to zero while D_4 and D_6 had greater negative bias due to significant deviations for Fraserdale, Ucluelet, and Whistler. Aside from these three sites, the D_4 predictions generally agreed well with the measurements. These same three sites and Groton were also significantly under predicted for D_6 but other sites were within a factor of 2 of the measurements. Possible explanations for model deviation could be population errors (Ucluelet and Whistler are tourist destinations and the population dataset used did not include visitors), non-personal care product emissions, product transformation of higher molecular weight siloxanes to D_4 on sampling media (Kierkegaard and McLachlan, 2013; Krogseth et al., 2013a), or our boundary conditions could be underestimating Asian cVMS transport. Genualdi et al. (2011) hypothesized the high D_4 concentrations measured at Whistler and Ucluelet could be due to transport from Asia since D_4 concentrations were greatest at west coast locations and especially at high altitude sites.

Model overprediction for D_5 occurred for the Point Reyes and Bratt's Lake sites. Representation error is a likely cause of this, since the actual sampling sites were upwind of large population centers (San Francisco and Regina, SK) in these grid cells; at 36 km resolution, the upwind sampling sites and the downwind emission centers are not resolved. However, Point Reyes and Bratt's Lake D_4 and D_6 concentrations were close to the modeled values.

We also compare the 36 km CMAQ D_5 concentration results to values from the DEHM and BETR models. The BETR model did not report values for Ucluelet or Groton so those sites are not included. The D_5 modeling attempts were ordered from most skilled to least skilled by using the mean of the fractional bias and fractional error (in parenthesis) scores, CMAQ -0.03 (0.66), DEHM -0.53 (0.73), and BETR -0.81 (1.08). The CMAQ and DEHM models had similar performance for Fraserdale, Whistler, Ucluelet, and Point Reyes, while the urban areas (Downsview, Sydney (FL), and Groton) were better predicted in the CMAQ model. Bratt's Lake was overestimated compared to the DEHM model and may have to do with the greater influence of Regina, SK emissions due to improved model resolution. The differences in modeled concentrations are most likely due to higher spatial resolution for CMAQ (36 km) versus 150 km (DEHM), and 15° (BETR) resolutions.

3.3.3 Toronto Model Comparison

Multiple measurement and modeling studies have investigated cVMS concentrations in Toronto, Canada. Table 2 shows the mean and hourly range of cVMS concentrations in Toronto for each of the four months as simulated by the CMAQ model. Table 2 further includes the March 2010 – April 2011 measured concentrations as collected by both passive and active sampling (Ahrens et al., 2014), active sampling from March 2012 – June 2012 and passive sampling from July 2012 – October 2012 (Krogseth et al., 2013b), and passive sampling (April – June 2009) from the GAPS network (Genualdi et al., 2011). Finally, the BETR and DEHM modeled D_5 concentrations (Apr – Jun 2009) are also tabulated (Genualdi et al., 2011). The CMAQ results compared favorably to the Ahrens et al. (2014) measurements with CMAQ monthly averages that generally fell within the reported measurement concentration ranges. D_4 monthly averages were within a factor of 0.97 – 1.94, D_5 within a factor of 0.59 – 1.39, and D_6 within a factor of 0.33 – 0.78 of the yearly averaged active and passive sampling measurements. Comparing the range of concentrations, CMAQ 24-hour averaged ranges were 4.6 – 60.6 (D_4), 17.1 – 247.7 (D_5), and 0.74 – 11.13 (D_6) ng m^{-3} compared to Ahrens et al. (2014) 24-hour active sampling range of 2.8 – 77 (D_4), 15 – 247 (D_5), and 1.9 – 22 (D_6) ng m^{-3}. Similarly, good agreement was observed for the active and passive sampling measurements from Krogseth et al. (2013b), average April CMAQ D_4, D_5, and D_6 concentrations were a factor of 0.84, 0.88, and 0.67 respectively of the measured average, the concentration ranges were similar, with higher peak concentrations occurring for the measurements despite sampling for 2-3 days. For the passive samples of Krogseth et al. (2013b), July and October average CMAQ concentrations were 0.69 – 0.76 for D_4 and 0.95 – 1.04 for D_5 compared to the measurements. CMAQ April averages were 1.85, 1.49, and 0.59 times the Genualdi et al. (2011) measurements. Previous Toronto modeling predicted 6.5 ng m^{-3} (BETR) and 28 ng m^{-3} (DEHM) which were significantly lower than the spring CMAQ D_5 concentration of 81.6 ng m^{-3}. Overall, the CMAQ model was able to better predict the higher observed concentrations of Toronto, which again, can most likely be attributed to increased model resolution.

3.4 Compound Ratios

Cyclic siloxane product ratios can be used to gain insight into emission sources and OH photochemical aging (Ahrens et al., 2014; Kierkegaard and McLachlan, 2013; Krogseth et al., 2013b; Krogseth et al., 2013a; Yucuis et al., 2013; Navea et al., 2011). Figures 6 and 7 show the model-predicted seasonal plots of monthly averaged D_5/D_4 and D_6/D_5 product ratios. It is important to note that the modeling assumes D_4 and D_6 are emitted according to population density, at constant ratios relative to D_5 at all locations and times. Thus, these figures emphasize the influence of differences in chemical aging. Due to differences in OH reactivity rates, cyclic siloxane reactivity increases with Si-O chain length (more methyl groups) so that D_6 is the most reactive and D_4 the least (Atkinson, 1991). Therefore, siloxane ratios depend on emissions, exposure to OH, and relative reactivity rates. Mole ratios are plotted with the more reactive species as the numerator; as air masses move away from emission sources and are exposed to OH, the ratio decreases due to more rapid depletion of the more reactive species. This is evident in the D_5/D_4 and D_6/D_5 maps which show urban areas have the highest ratios.

Seasonal differences of the product ratios are similar for both D_5/D_4 and D_6/D_5 mole ratios. Urban areas exhibit almost no season-to-season difference (Table S7), as they reflect the local emission ratios. Seasonal differences are most apparent for rural and remote locations. Domain average ratios are highest in January and lowest in July which is consistent with seasonal OH fluctuations.

Since both SO_2 and cVMS are precursors to secondary aerosol formation, and both compounds have approximately the same OH rate constant, the ratio of gas phase SO_2 to cVMS should predict aerosol-phase ratios of S to Si in photochemically generated particles (Bzdek et al., 2014). Figure 8 shows the seasonally modeled, monthly averaged gas phase $SO_2/(D_4 + D_5 + D_6)$ mole ratios. Urban ratios exhibit lowest values which suggest photochemically generated aerosols would have increased Si composition derived from siloxane oxidation. Conversely, rural locations have high SO_2/cVMS ratios and expected low Si aerosol composition. This is consistent with the high nanoparticle Si measured in Pasadena, CA and Lewes, DE by Bzdek et al. (2014). Seasonal variation in the SO_2/cVMS ratio is minor.

3.5 Vertical profile analysis

Modeled monthly averaged D_5 and o-D_5 vertical profiles are shown in Figure 9 for three grid cells near Los Angeles. The locations of the analyzed sites include the highest monthly averaged surface July D_5 concentration, the highest averaged surface o-D_5 concentration, and a grid cell over the Pacific Ocean. The grid cell with greatest D_5 concentration, (termed "Peak D_5") included cities such as Long Beach and Anaheim while the grid cell with highest o-D_5 ("Peak o-D_5") was approximately 80 km northeast of the peak D_5 grid cell and included Victorville and Hesperia, CA. The third location was over the Pacific Ocean ("Pacific") approximately 195 km southwest of Los Angeles (Fig. S9).

The CMAQ model was run with 14 vertical layers; plotted is the layer top height versus the monthly averaged July D_5 and o-D_5 concentration. For D_5 concentrations, both the "Peak D_5" and "Peak o-D_5" sites had highest concentrations at the surface. Over the Pacific, concentrations peaked above the surface at approximately 700-1,700 m. Surface D_5 concentrations

were 251, 103, and 0.3 ng m^{-3} for the "Peak D$_5$", "Peak o-D$_5$", and "Pacific" locations respectively. From heights 475-3,000 m, the "Peak o-D$_5$" site had higher D$_5$ concentrations than the "Peak D$_5$" site and this is most likely due to the plume dilution from the upwind LA source. For o-D$_5$ concentrations, surface concentrations were highest for the "Peak o-D$_5$" site (9 ng m^{-3}), followed by the "Peak D$_5$" site (2 ng m^{-3}), and the "Pacific" site (0.2 ng m^{-3}). From the surface to 3,000 m the "Peak o-D$_5$" grid cell had highest o-D$_5$ concentrations as a result of being downwind of a major emission source and the oxidation reaction takes times to occur. Both the "Peak D$_5$" and "Pacific" sites have peak o-D$_5$ concentrations not at the surface (475 and 2,300 meters respectively) while the "o-D$_5$" site is at the surface. The low surface o-D$_5$ at the peak D$_5$ site could be due to low OH concentrations caused by urban OH sinks and is consistent with low modeled surface OH (Fig. S10). Vertical concentrations appear to be dependent on transport, reaction time, and OH concentrations.

4 Conclusions

The CMAQ model was modified to include D$_4$, D$_5$, D$_6$, and the oxidation products to investigate urban-rural concentration gradients, seasonal variability, product and SO$_2$ mole ratios, and vertical profiles. Improved model performance was observed when compared to previous modeling especially for urban areas. Concentrations are heavily dependent on population with strong urban/rural concentration gradients observed. Urban areas have highest cVMS concentrations but are not significantly influenced by seasonal variability of OH, while rural cVMS is influenced by transport and regional OH concentrations. The oxidized product concentrations are significantly lower than the parent compounds with average D$_5$ concentrations up to 432 ng m^{-3} and average o-D$_5$ up to 9 ng m^{-3}. Highest oxidized siloxane concentrations occur downwind of major urban centers. Increased error for modeled D$_4$ and D$_6$ relative to D$_5$ is hypothesized to be due to increased uncertainty in emission estimates. Future work should address these emission uncertainties by exploring seasonal, temporal, spatial, and non-personal care product emissions.

While the parent compounds have been extensively studied, the environmental and health impact of the oxidized species have not been addressed. This is especially important since the oxidation products likely form particles. To the best of our knowledge this work provides the first estimated atmospheric loadings and spatial distribution of the oxidized species. Future work should focus on gas and particle phase measurements of the oxidized species to confirm particle formation in the ambient environment and to determine typical loadings in the environment. This is especially important since exposure would be expected to be highest indoors where cyclic siloxane concentrations are greatest.

Competing Interests

The authors declare that they have no conflict of interest.

References

Ahrens, L., Harner, T., and Shoeib, M.: Temporal variations of cyclic and linear volatile methylsiloxanes in the atmosphere using passive samplers and high-volume air samplers, Environ. Sci. Technol., 48, 9374-9381, doi:10.1021/es502081j, 2014.

Atkinson, R.: Kinetics of the Gas-Phase Reactions of a Series of Organosilicon Compounds with OH and NO3 Radicals and O3 at 297 +/- 2 K, Environ. Sci. Technol., 25, 863-866, doi:10.1021/es00017a005, 1991.

Brooke, D., Crookes, M., Gray, D., and Robertson, S.: Environmental Risk Assessment Report: Dodecamethylcyclohexasiloxane, Environment Agency of England and Wales, Bristol, UK, 2009a.

Brooke, D., Crookes, M., Gray, D., and Robertson, S.: Environmental Risk Assessment Report: Decamethylcyclopentasiloxane, Environment Agency of England and Wales, Bristol, UK, 2009b.

Brooke, D., Crookes, M., Gray, D., and Robertson, S.: Environmental Risk Assessment Report: Octamethylcyclotetrasiloxane, Environment Agency of England and Wales, Bristol, UK, 2009c.

Buser, A. M., Kierkegaard, A., Bogdal, C., MacLeod, M., Scheringer, M., and Hungerbuhler, K.: Concentrations in Ambient Air and Emissions of Cyclic Volatile Methylsiloxanes in Zurich, Switzerland, Environ. Sci. Technol., 47, 7045-7051, doi:10.1021/es3046586, 2013a.

Buser, A. M., Schenker, S., Scheringer, M., and Hungerbühler, K.: Comparing the Performance of Computational Estimation Methods for Physicochemical Properties of Dimethylsiloxanes and Selected Siloxanols, J. Chem. Eng. Data, 58, 3170-3178, doi:10.1021/je400633h, 2013b.

Buser, A. M., Bogdal, C., MacLeod, M., and Scheringer, M.: Emissions of decamethylcyclopentasiloxane from Chicago, Chemosphere, 107, 473-475, doi:10.1016/j.chemosphere.2013.12.034, 2014.

Byun, D., and Schere, K. L.: Review of the governing equations, computational algorithms, and other components of the models-3 Community Multiscale Air Quality (CMAQ) modeling system, Appl. Mech. Rev., 59, 51-77, doi:10.1115/1.2128636, 2006.

Byun, D. W., Pleim, J. E., Tang, R. T., and Bourgeois, A.: Chapter 12: Meteorology-Chemistry Interface Processor (MCIP) for Models-3 Community Multiscale Air Quality (CMAQ) Modeling System, in: Science Algorithms of the EPA Models-3 Community Multiscale Air Quality (CMAQ) Modeling System, United States Environmental Protection Agency, Washington, DC, 1999.

Bzdek, B. R., Horan, A. J., Pennington, M. R., Janechek, N. J., Baek, J., Stanier, C. O., and Johnston, M. V.: Silicon is a Frequent Component of Atmospheric Nanoparticles, Environ. Sci. Technol., 48, 11137-11145, doi:10.1021/es5026933, 2014.

Capela, D., Alves, A., Homem, V., and Santos, L.: From the shop to the drain - Volatile methylsiloxanes in cosmetics and personal care products, Environ. Int., 92-93, 50-62, doi:10.1016/j.envint2016.03.016, 2016.

Chandramouli, B., and Kamens, R. M.: The photochemical formation and gas-particle partitioning of oxidation products of decamethyl cyclopentasiloxane and decamethyl tetrasiloxane in the atmosphere, Atmos. Environ., 35, 87-95, doi:10.1016/s1352-2310(00)00289-2, 2001.

Cheng, Y., Shoeib, M., Ahrens, L., Harner, T., and Ma, J.: Wastewater treatment plants and landfills emit volatile methyl siloxanes (VMSs) to the atmosphere: Investigations using a new passive air sampler, Environ. Pollut., 159, 2380-2386, doi:10.1016/j.envpol.2011.07.002, 2011.

Companioni-Damas, E. Y., Santos, F. J., and Galceran, M. T.: Linear and cyclic methylsiloxanes in air by concurrent solvent recondensation-large volume injection-gas chromatography-mass spectrometry, Talanta, 118, 245-252, doi:10.1016/j.talanta.2013.10.020, 2014.

Dudzina, T., von Goetz, N., Bogdal, C., Biesterbos, J. W. H., and Hungerbuhler, K.: Concentrations of cyclic volatile methylsiloxanes in European cosmetics and personal care products: Prerequisite for human and environmental exposure assessment, Environ. Int., 62, 86-94, doi:10.1016/j.envint.2013.10.002, 2014.

ECHA: Annex XV Restriction Report Proposal for a Restriction (D4 and D5), Health & Safety Executive, Bootle, UK, 2015.

Environment Canada and Health Canada: Screening Assessment for the Challenge Octamethylcyclotetrasiloxane (D4), 2008a.

Environment Canada and Health Canada: Screening Assessment for the Challenge Decamethylcyclopentasiloxane (D5), 2008b.

Environment Canada and Health Canada: Screening Assessment for the Challenge Dodecamethylcyclohexasiloxane (D6), 2008c.

EPA: Estimation Programs Interface Suite for Microsoft Windows, v 4.11, United States Environmental Protection Agency, Washington, DC, USA., 2012.

Fairbrother, A., Burton, G. A., Klaine, S. J., Powell, D. E., Staples, C. A., Mihaich, E. M., Woodburn, K. B., and Gobas, F. A. P. C.: Characterization of ecological risks from environmental releases of decamethylcyclopentasiloxane (D5), Environ. Toxicol. Chem., 34, 2715-2722, doi:10.1002/etc.3041, 2015.

Genualdi, S., Harner, T., Cheng, Y., MacLeod, M., Hansen, K. M., van Egmond, R., Shoeib, M., and Lee, S. C.: Global Distribution of Linear and Cyclic Volatile Methyl Siloxanes in Air, Environ. Sci. Technol., 45, 3349-3354, doi:10.1021/es200301j, 2011.

Gobas, F. A. P. C., Powell, D. E., Woodburn, K. B., Springer, T., and Huggett, D. B.: Bioaccumulation of decamethylpentacyclosiloxane (D5): A review, Environ. Toxicol. Chem., 34, 2703-2714, doi:10.1002/etc.3242, 2015a.

Gobas, F. A. P. C., Xu, S., Kozerski, G., Powell, D. E., Woodburn, K. B., Mackay, D., and Fairbrother, A.: Fugacity and activity analysis of the bioaccumulation and environmental risks of decamethylcyclopentasiloxane (D5), Environ. Toxicol. Chem., 34, 2723-2731, doi:10.1002/etc.2942, 2015b.

Gouin, T., van Egmond, R., Sparham, C., Hastie, C., and Chowdhury, N.: Simulated use and wash-off release of decamethylcyclopentasiloxane used in anti-perspirants, Chemosphere, 93, 726-734, doi:10.1016/j.chemosphere.2012.10.042, 2013.

Hansen, K. M., Christensen, J. H., Brandt, J., Frohn, L. M., Geels, C., Skjoth, C. A., and Li, Y.-F.: Modeling short-term variability of alpha-hexachlorocyclohexane in Northern Hemispheric air, J. Geophys. Res.-Atmos., 113, doi:10.1029/2007jd008492, 2008.

5 Horii, Y., and Kannan, K.: Survey of organosilicone compounds, including cyclic and linear siloxanes, in personal-care and household products, Arch. Environ. Con. Tox., 55, 701-710, doi:10.1007/s00244-008-9172-z, 2008.

Kierkegaard, A., and McLachlan, M. S.: Determination of linear and cyclic volatile methylsiloxanes in air at a regional background site in Sweden, Atmos. Environ., 80, 322-329, doi:10.1016/j.atmosenv.2013.08.001, 2013.

Kim, J., and Xu, S.: Sorption and desorption kinetics and isotherms of volatile methylsiloxanes with atmospheric aerosols, Chemosphere,
10 144, 555-563, doi:10.1016/j.chemosphere.2015.09.033, 2016.

Krogseth, I. S., Kierkegaard, A., McLachlan, M. S., Breivik, K., Hansen, K. M., and Schlabach, M.: Occurrence and Seasonality of Cyclic Volatile Methyl Siloxanes in Arctic Air, Environ. Sci. Technol., 47, 502-509, doi:10.1021/es3040208, 2013a.

Krogseth, I. S., Zhang, X. M., Lei, Y. D., Wania, F., and Breivik, K.: Calibration and Application of a Passive Air Sampler (XAD-PAS) for Volatile Methyl Siloxanes, Environ. Sci. Technol., 47, 4463-4470, doi:10.1021/es400427h, 2013b.

15 Latimer, H. K., Kamens, R. M., and Chandra, G.: The Atmospheric Partitioning of Decamethylcylcopentasiloxane (D5) and 1-Hydroxynonomethylcyclopentasiloxane (D4TOH) on Different Types of Atmospheric Particles, Chemosphere, 36, 2401-2414, doi:10.1016/S0045-6535(97)10209-0, 1998.

Lei, Y. D., Wania, F., and Mathers, D.: Temperature-Dependent Vapor Pressure of Selected Cyclic and Linear Polydimethylsiloxane Oligomers, J. Chem. Eng. Data, 55, 5868-5873, doi:10.1021/je100835n, 2010.

20 Lu, Y., Yuan, T., Wang, W., and Kannan, K.: Concentrations and assessment of exposure to siloxanes and synthetic musks in personal care products from China, Environ. Pollut., 159, 3522-3528, doi:10.1016/j.envpol.2011.08.015, 2011.

Lyman, W. J., Reehl, W. F., and Rosenblatt, D. H.: Handbook of Chemical Property Estimation Methods: Environmental Behavior of Organic Compounds, McGraw-Hill, New York City, 1982.

Mackay, D., Cowan-Ellsberry, C. E., Powell, D. E., Woodburn, K. B., Xu, S., Kozerski, G. E., and Kim, J.: Decamethylcyclopentasiloxane
25 (D5) environmental sources, fate, transport, and routes of exposure, Environ. Toxicol. Chem., 34, 2689-2702, doi:10.1002/etc.2941, 2015.

MacLeod, M., von Waldow, H., Tay, P., Armitage, J. M., Wohrnschimmel, H., Riley, W. J., McKone, T. E., and Hungerbuhler, K.: BETR global - A geographically-explicit global-scale multimedia contaminant fate model, Environ. Pollut., 159, 1442-1445, doi:10.1016/j.envpol.2011.01.038, 2011.

McLachlan, M. S., Kierkegaard, A., Hansen, K. M., van Egmond, R., Christensen, J. H., and Skjoth, C. A.: Concentrations and Fate of
30 Decamethylcyclopentasiloxane (D-5) in the Atmosphere, Environ. Sci. Technol., 44, 5365-5370, doi:10.1021/es100411w, 2010.

Montemayor, B. P., Price, B. B., and van Egmond, R. A.: Accounting for intended use application in characterizing the contributions of cyclopentasiloxane (D5) to aquatic loadings following personal care product use: antiperspirants, skin care products and hair care products, Chemosphere, 93, 735-740, doi:10.1016/j.chemosphere.2012.10.043, 2013.

Navea, J. G., Xu, S., Stanier, C. O., Young, M. A., and Grassian, V. H.: Effect of Ozone and Relative Humidity on the Heterogeneous Uptake
35 of Octamethylcyclotetrasiloxane and Decamethylcyclopentasiloxane on Model Mineral Dust Aerosol Components, J. Phys. Chem. A, 113, 7030-7038, doi:10.1021/jp902192b, 2009a.

Navea, J. G., Xu, S. H., Stanier, C. O., Young, M. A., and Grassian, V. H.: Heterogeneous uptake of octamethylcyclotetrasiloxane (D-4) and decamethylcyclopentasiloxane (D-5) onto mineral dust aerosol under variable RH conditions, Atmos. Environ., 43, 4060-4069, doi:10.1016/j.atmosenv.2009.05.012, 2009b.

40 Navea, J. G., Young, M. A., Xu, S., Grassian, V. H., and Stanier, C. O.: The atmospheric lifetimes and concentrations of cyclic methylsiloxanes octamethylcyclotetrasiloxane (D(4)) and decamethylcyclopentasiloxane (D(5)) and the influence of heterogeneous uptake, Atmos. Environ., 45, 3181-3191, doi:10.1016/j.atmosenv.2011.02.038, 2011.

OECD Environment Directorate: The 2004 OECD List of High Production Volume Chemicals, 2004.

Pieri, F., Katsoyiannis, A., Martellini, T., Hughes, D., Jones, K. C., and Cincinelli, A.: Occurrence of linear and cyclic volatile methyl
45 siloxanes in indoor air samples (UK and Italy) and their isotopic characterization, Environ. Int., 59, 363-371, doi:10.1016/j.envint.2013.06.006, 2013.

Roselle, S. J., and Binkowski, F. S.: Chapter 11: Cloud Dynamics and Chemistry, in: Science Algorithms of the EPA Models-3 Community Multiscale Air Quality (CMAQ) Modeling System, United States Environmental Protection Agency, Washington, DC, 1999.

Rucker, C., and Kummerer, K.: Environmental chemistry of organosiloxanes, Chem. Rev., 115, 466-524, doi:10.1021/cr500319v, 2015.

50 Shoeib, M., and Harner, T.: Using measured octanol-air partition coefficients to explain environmental partitioning of organochlorine pesticides, Environ. Toxicol. Chem., 21, 984-990, doi:10.1002/etc.5620210513, 2002.

Slowik, J. G., Brook, J., Chang, R. Y. W., Evans, G. J., Hayden, K., Jeong, C. H., Li, S. M., Liggio, J., Liu, P. S. K., McGuire, M., Mihele, C., Sjostedt, S., Vlasenko, A., and Abbatt, J. P. D.: Photochemical processing of organic aerosol at nearby continental sites: contrast between urban plumes and regional aerosol, Atmos. Chem. Phys., 11, 2991-3006, doi:10.5194/acp-11-2991-2011, 2011.

Sommerlade, R., Parlar, H., Wrobel, D., and Kochs, P.: Product Analysis and Kinetics of the Gas-Phase Reactions of Selected Organosilicon Compounds with OH Radicals Using a Smog Chamber - Mass Spectrometer System, Environ. Sci. Technol., 27, 2435-2440, doi:10.1021/es00048a019, 1993.

Spak, S., Baek, J., Carlson, J., Carmichael, G. R., Kim, Y. J., Riemer, N., and Stanier, C.: Episodic Air Pollution in Wisconsin (LADCO Winter Nitrate Study) and Georgia (SEARCH Network) During Jan–Mar 2009, Phase II Report, Three Dimensional Modeling, Process Analysis, and Emissions Sensitivity, Lake Michigan Air Directors Consortium, Rosemont, IL, 2012.

Spivakovsky, C. M., Logan, J. A., Montzka, S. A., Balkanski, Y. J., Foreman-Fowler, M., Jones, D. B. A., Horowitz, L. W., Fusco, A. C., Brenninkmeijer, C. A. M., Prather, M. J., Wofsy, S. C., and McElroy, M. B.: Three-dimensional climatological distribution of tropospheric OH: Update and evaluation, J. Geophys. Res.-Atmos., 105, 8931-8980, doi:10.1029/1999jd901006, 2000.

Tang, X., Misztal, P. K., Nazaroff, W. W., and Goldstein, A. H.: Siloxanes Are the Most Abundant Volatile Organic Compound Emitted from Engineering Students in a Classroom, Environ. Sci. Technol. Lett., 2, 303-307, doi:10.1021/acs.estlett.5b00256, 2015.

Tri Manh, T., Abualnaja, K. O., Asimakopoulos, A. G., Covaci, A., Gevao, B., Johnson-Restrepo, B., Kumosani, T. A., Malarvannan, G., Tu Binh, M., Moon, H.-B., Nakata, H., Sinha, R. K., and Kannan, K.: A survey of cyclic and linear siloxanes in indoor dust and their implications for human exposures in twelve countries, Environ. Int., 78, 39-44, doi:10.1016/j.envint.2015.02.011, 2015.

Tri Manh, T., and Kannan, K.: Occurrence of cyclic and linear siloxanes in indoor air from Albany, New York, USA, and its implications for inhalation exposure, Sci. Total Environ., 511, 138-144, doi:10.1016/j.scitotenv.2014.12.022, 2015.

van Egmond, R.: Personal Communication to C. O. Stanier, 16 October, 2013.

Wang, D. G., Norwood, W., Alaee, M., Byer, J. D., and Brimble, S.: Review of recent advances in research on the toxicity, detection, occurrence and fate of cyclic volatile methyl siloxanes in the environment, Chemosphere, 93, 711-725, doi:10.1016/j.chemosphere.2012.10.041, 2013.

Wang, R., Moody, R. P., Koniecki, D., and Zhu, J.: Low molecular weight cyclic volatile methylsiloxanes in cosmetic products sold in Canada: implication for dermal exposure, Environ. Int., 35, 900-904, doi:10.1016/j.envint.2009.03.009, 2009.

Wang, X. M., Lee, S. C., Sheng, G. Y., Chan, L. Y., Fu, J. M., Li, X. D., Min, Y. S., and Chan, C. Y.: Cyclic organosilicon compounds in ambient air in Guangzhou, Macau and Nanhai, Pearl River Delta, Appl. Geochem., 16, 1447-1454, doi:10.1016/S0883-2927(01)00044-0, 2001.

Wania, F.: Assessing the potential of persistent organic chemicals for long-range transport and accumulation in polar regions, Environ. Sci. Technol., 37, 1344-1351, doi:10.1021/es026019e, 2003.

Whelan, M. J., Estrada, E., and van Egmond, R.: A modelling assessment of the atmospheric fate of volatile methyl siloxanes and their reaction products, Chemosphere, 57, 1427-1437, doi:10.1016/j.chemosphere.2004.08.100, 2004.

Wu, Y., and Johnston, M. V.: Molecular Characterization of Secondary Aerosol from Oxidation of Cyclic Methylsiloxanes, J. Am. Soc. Mass. Spectr., 27, 402-409, doi:10.1007/s13361-015-1300-1, 2016.

Xu, S., and Kropscott, B.: Method for simultaneous determination of partition coefficients for cyclic volatile methylsiloxanes and dimethylsilanediol, Anal. Chem., 84, 1948-1955, doi:10.1021/ac202953t, 2012.

Xu, S., and Wania, F.: Chemical fate, latitudinal distribution and long-range transport of cyclic volatile methylsiloxanes in the global environment: a modeling assessment, Chemosphere, 93, 835-843, doi:10.1016/j.chemosphere.2012.10.056, 2013.

Yucuis, R. A., Stanier, C. O., and Hornbuckle, K. C.: Cyclic siloxanes in air, including identification of high levels in Chicago and distinct diurnal variation, Chemosphere, 92, 905-910, doi:10.1016/j.chemosphere.2013.02.051, 2013.
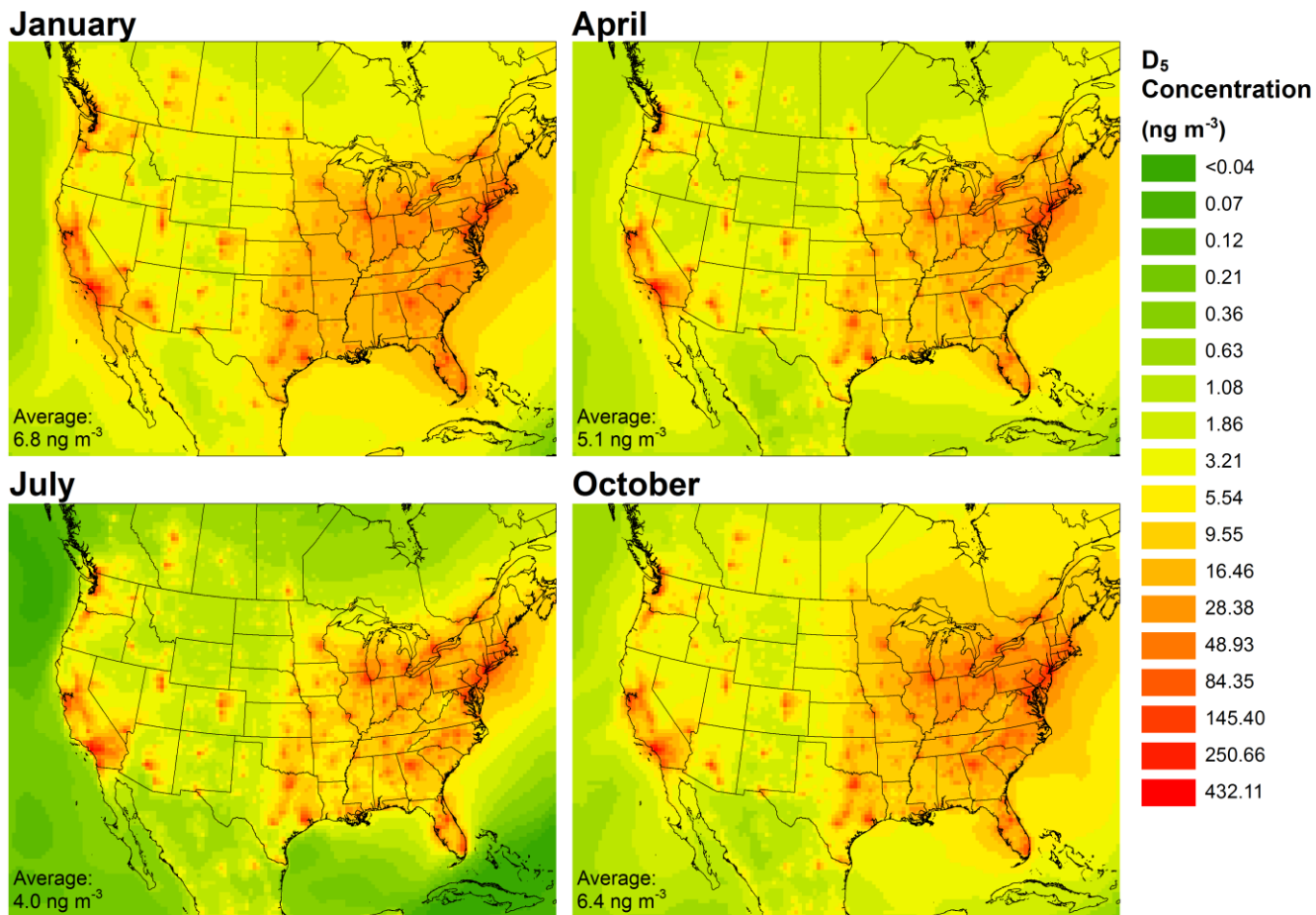
Figure 1: Monthly averaged surface layer D₅ concentrations. The domain average concentration is shown in the lower left for each month.
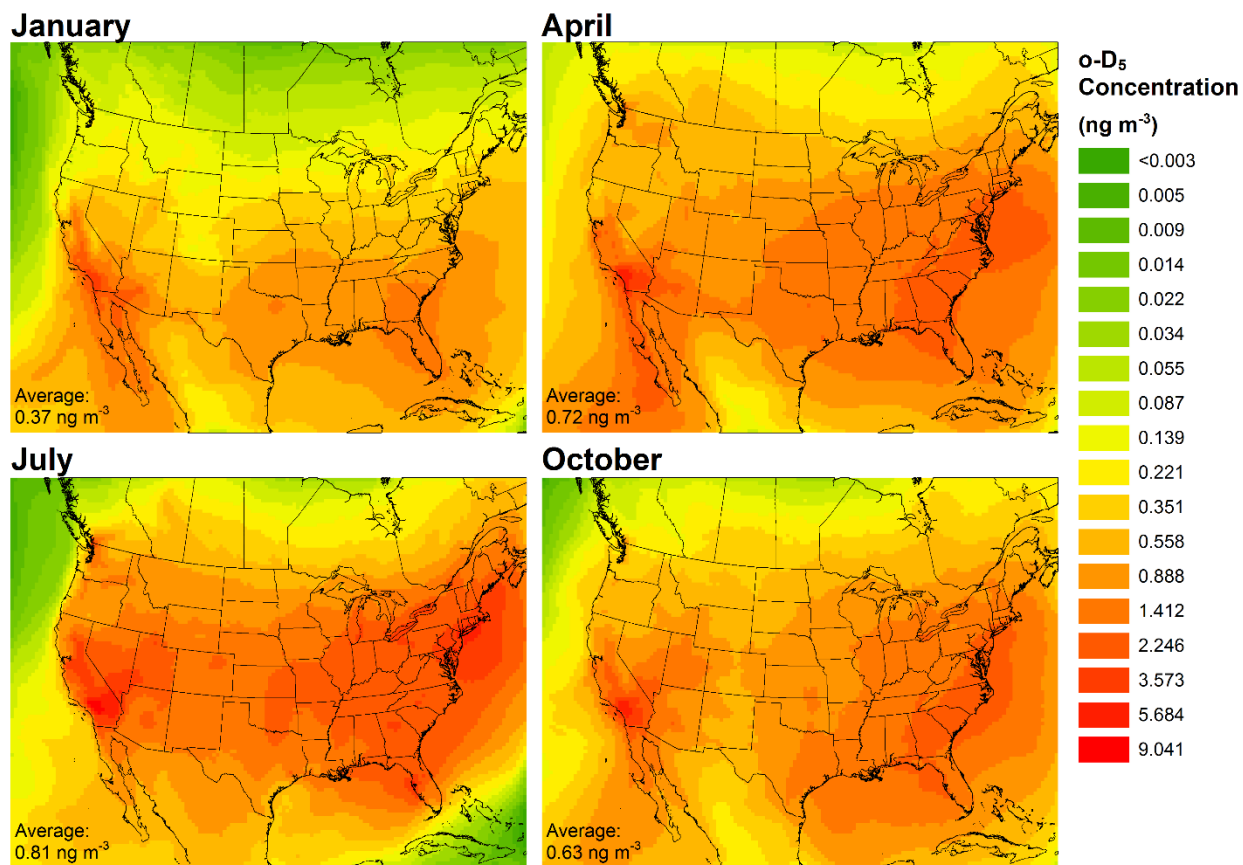
Figure 2: Monthly average surface layer oxidized D_5 (o-D_5) concentrations. The domain average concentration is shown in the lower left for each month.

Table 1: Monthly minimum, maximum, and average D_5 and o-D_5 concentrations in the lowest modeled layer for the domain.

Domain	D_5 Concentrations (ng m^{-3})				o-D_5 Concentrations (ng m^{-3})			
	January	April	July	October	January	April	July	October
Minimum	0.14	0.27	0.024	0.27	0.0031	0.037	0.0021	0.0033
Maximum	432	379	265	301	3.19	4.86	9.04	5.21
Average	6.82	5.09	4.04	6.43	0.37	0.72	0.81	0.63
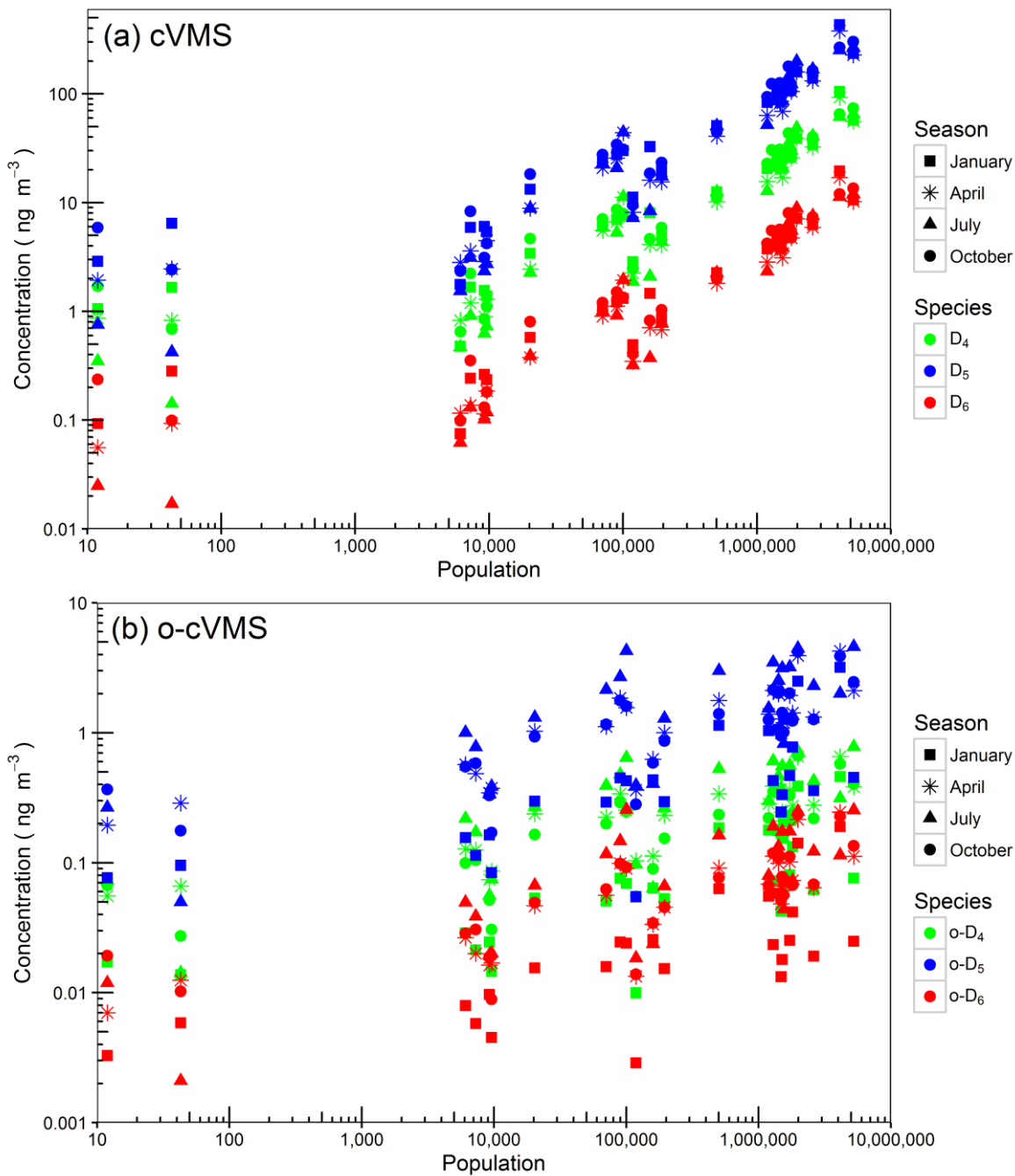
Figure 3: Average monthly CMAQ modeled surface (a) cVMS and (b) oxidized cVMS concentrations are plotted versus 36-km grid cell population for 26 U.S. and Canadian sites. These sites include the ten most populous U.S. metropolitan areas, previous siloxane measurement sites, and NOAA Climate Monitoring and Diagnostics Laboratory (CMDL) sites. See Table S3 for the listing of these sites.
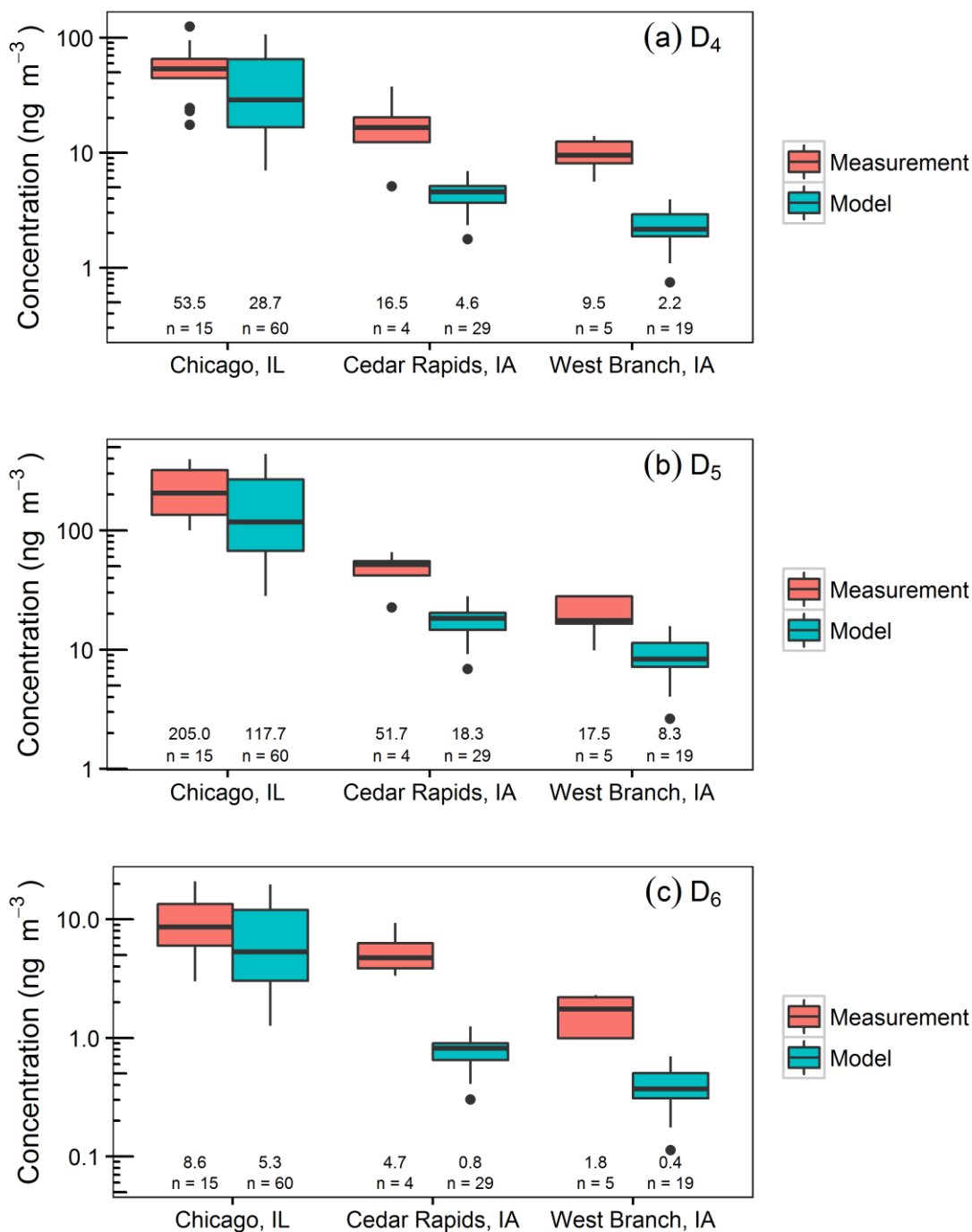
Figure 4: Model comparison to Yucuis et al. (2013). Model results from CMAQ (July 1-30 simulation); measurements were conducted in 2011 from Aug 13-21 (Chicago), Jun 29-Jul 26 (Cedar Rapids), and Jul 6-22 (West Branch), respectively. Hourly model data was averaged to 12, 24, and 36 hour periods, starting at typical measurement start times. Median concentrations and number of observations are tabulated under the boxplots.
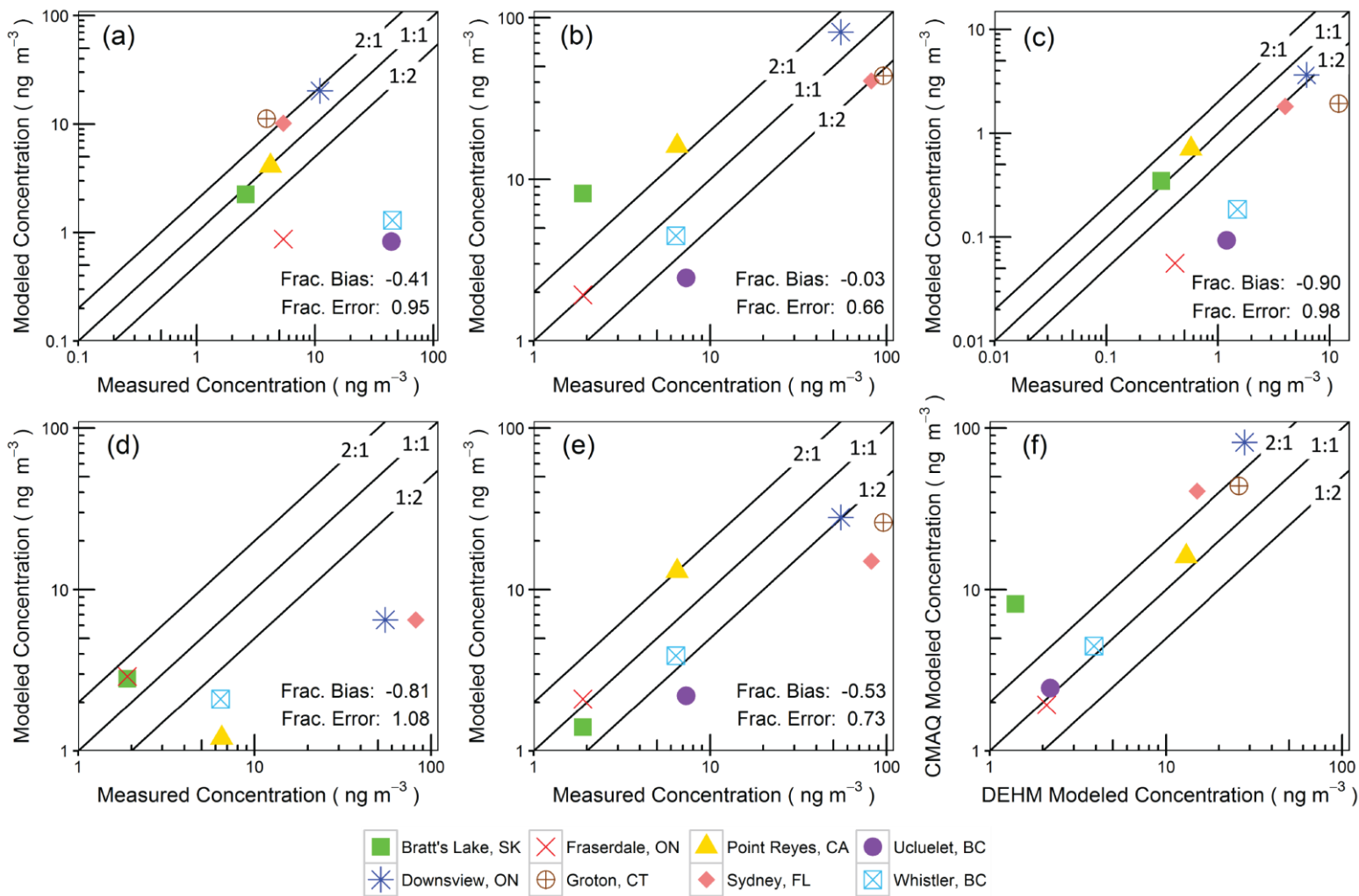
Figure 5: Plot (a) shows CMAQ D₄, (b) CMAQ D₅, (c) CMAQ D₆, (d) BETR D₅, and (e) DEHM D₅ modeled concentrations compared to Genualdi et al. (2011) measurements. Plot (f) compares modeled CMAQ D₅ versus DEHM D₅ concentrations. CMAQ model results are the April averaged concentrations while BETR and DEHM model results are from Genualdi et al. (2011) and represent the same period as the measurements. CMAQ model resolution was 36 km, DEHM 150 km, and BETR 15°.

23

Table 2: Toronto cyclic siloxane comparison between the CMAQ model and previous studies. Reported is the mean concentration with the range in parenthesis.

Period	Method	Averaging Period	D_4 (ng m^{-3})	D_5 (ng m^{-3})	D_6 (ng m^{-3})	Reference
			Atmospheric Concentration, mean (range)			
January	CMAQ Model	24 h	21.7 (5.4 - 45.1)	88.1 (21.5 - 184.8)	3.94 (0.95 - 8.31)	*This study*
April	CMAQ Model	24 h	20.4 (4.6 - 43.7)	82.1 (17.1 - 178.2)	3.67 (0.74 - 8.01)	*This study*
July	CMAQ Model	24 h	28.3 (7.5 - 57.0)	115.9 (30.5 - 233.8)	5.22 (1.37 - 10.54)	*This study*
October	CMAQ Model	24 h	31.0 (5.4 - 60.6)	126.3 (20.8 -247.7)	5.67 (0.90 - 11.13)	*This study*
March 2010 - April 2011	Active sampling	24 h (not continuous)	16 (2.8 - 77)	91 (15 - 247)	7.3 (1.9 - 22)	*Ahrens et al. (2014)*
March 2010 - April 2011	Passive sampling	~28 d	21 (9.3 - 35)	140 (89 - 168)	11 (8.0 - 20)	*Ahrens et al. (2014)*
March 2012 - June 2012	Active sampling	2-3 d	24.2 (4.7 - 90.9)	93.5 (22.4 - 355)	5.5 (1.6 - 17.4)	*Krogseth et al. (2013b)*
July 2012 - October 2012	Passive sampling	80-92 d	41	122	-	*Krogseth et al. (2013b)*
April 2009 - June 2009	Passive sampling	89 d	11	55	6.2	*Genualdi et al. (2011)*
April 2009 - June 2009	BETR Model	89 d	-	6.5	-	*Genualdi et al. (2011)*
April 2009 - June 2009	DEHM Model	89 d	-	28	-	*Genualdi et al. (2011)*
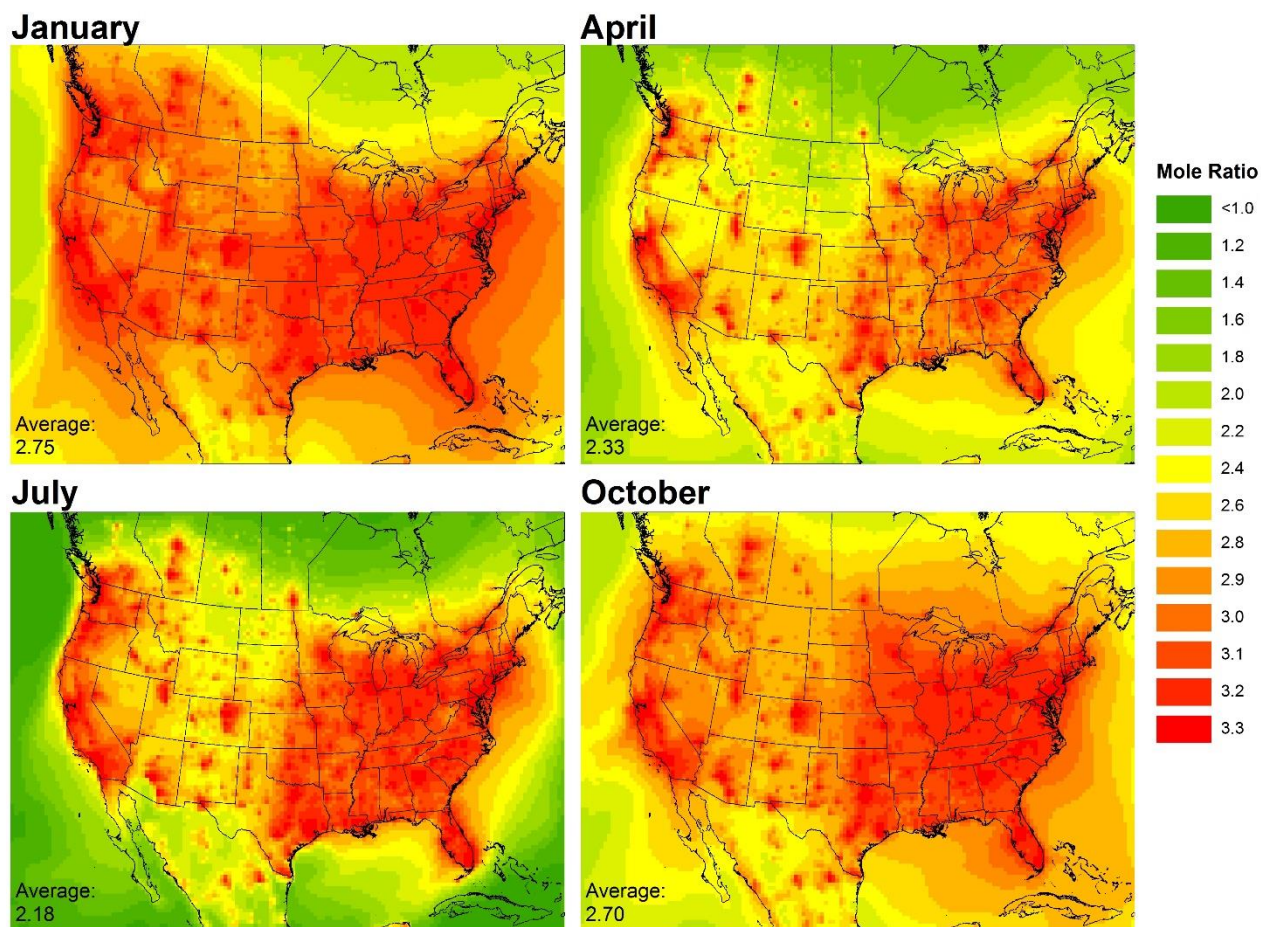
Figure 6: Modeled monthly averaged D_5/D_4 mole ratios by season. Larger cVMS species react faster with OH. More reactive species are in the numerator; therefore, ratios decrease with air mass age.
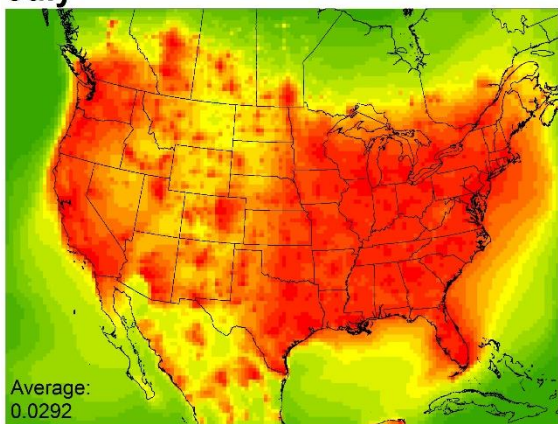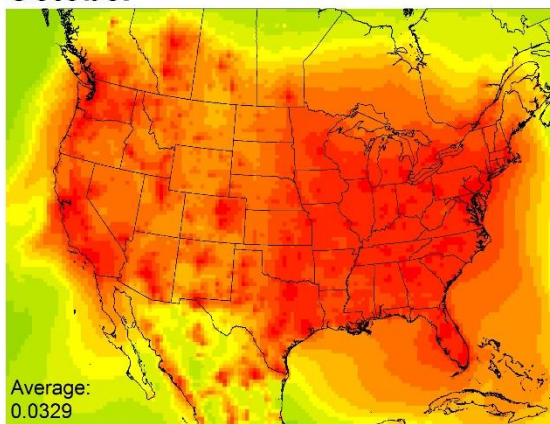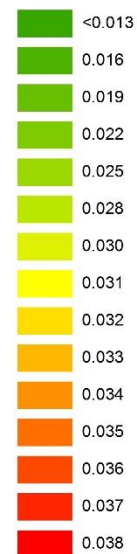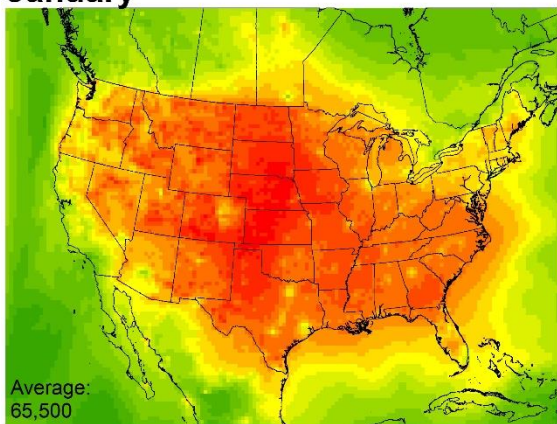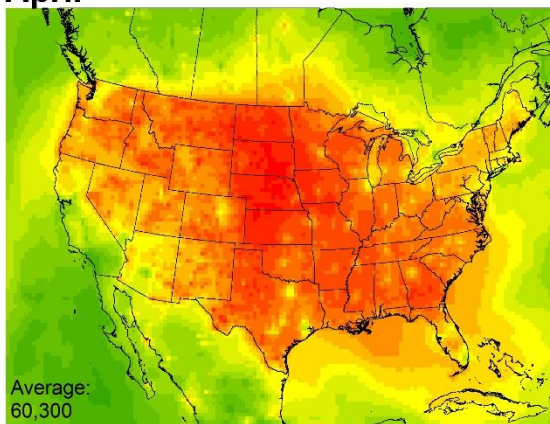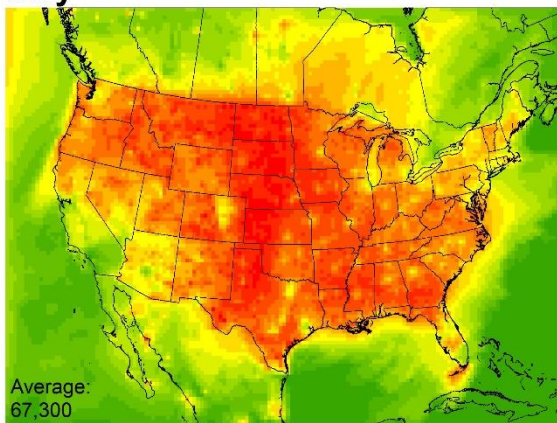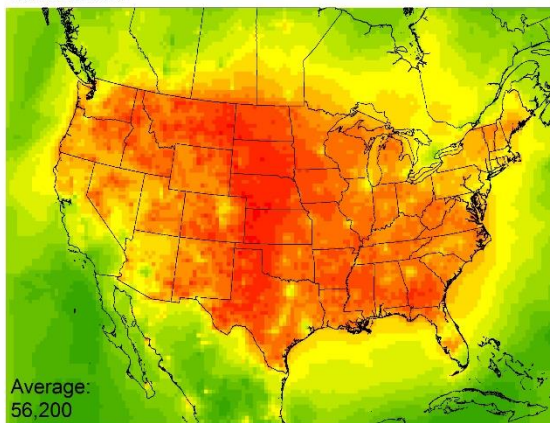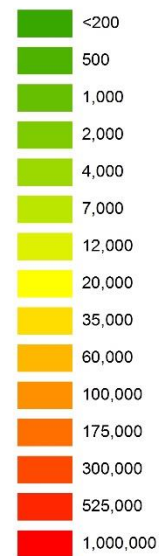
5
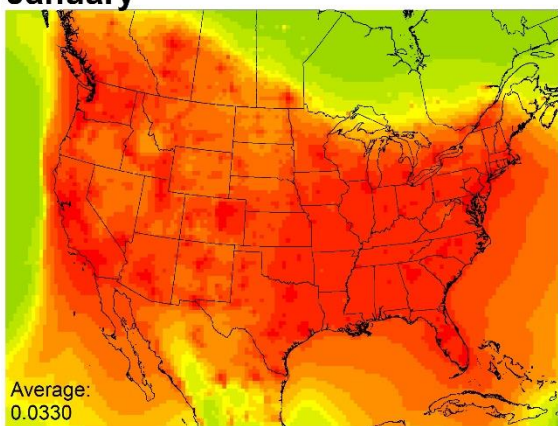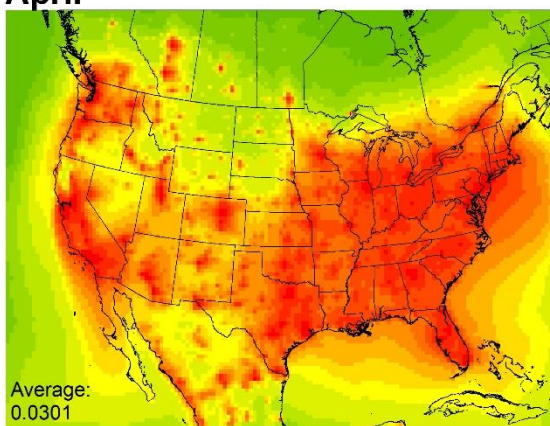
Figure 7: Modeled monthly averaged D_6/D_5 mole ratios by season. Larger cVMS species react faster with OH. More reactive species are in the numerator; therefore, ratios decrease with air mass age.

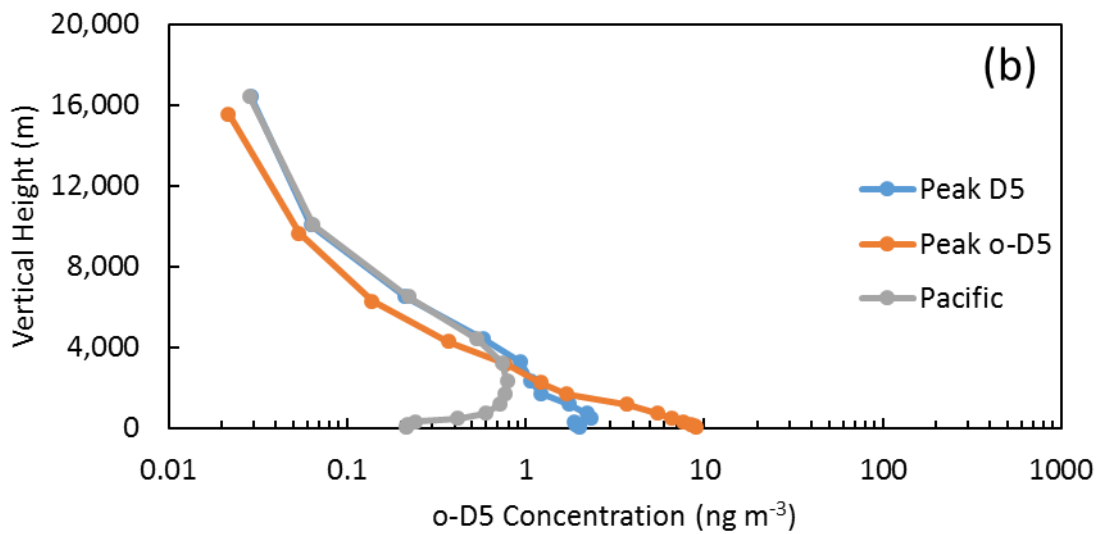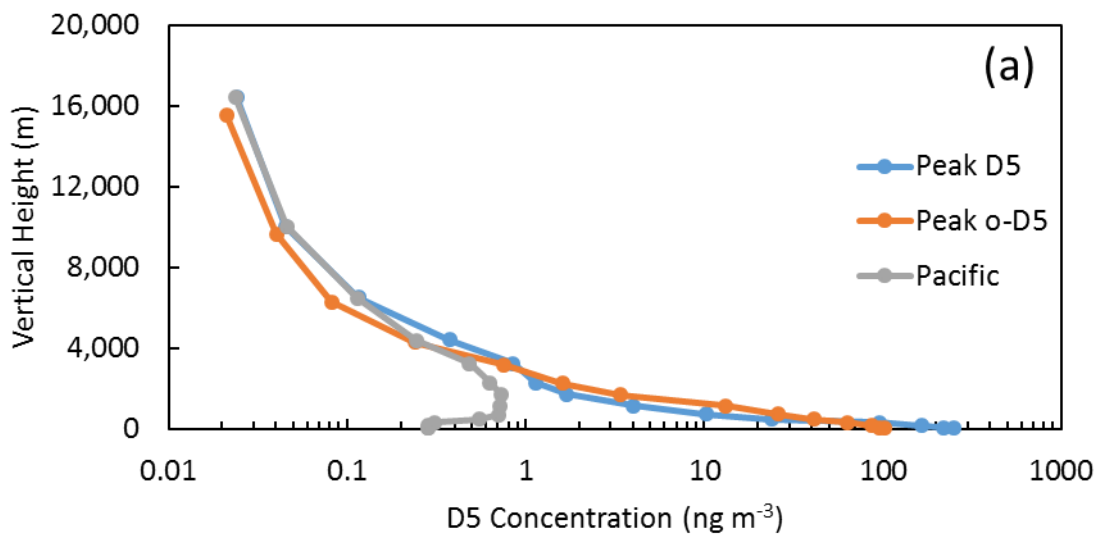**Figure 8: Modeled monthly averaged SO$_2$/ (D$_4$+D$_5$+D$_6$) mole ratio by season.**

Figure 9: Monthly averaged vertical profiles for grid cells near Los Angeles. Plot (a) shows D_5 and (b) o-D_5 model concentrations. Grid cells refer to the location of maximum July D_5, maximum July o-D_5, and a grid cell over the Pacific Ocean.